Harmonic mode-locking fiber ring laser with a pulse repetition rate up to 12 GHz

Korobko D.A.[1*], Stoliarov D.A.[1], Itrin P.A.[1], Odnoblyudov M.A.[2], Petrov A.B.[2, 3] and Gumenyuk R.V.[1,4]

[1]Ulyanovsk State University, 42 Leo Tolstoy Street, 432017, Ulyanovsk, Russian Federation;
[2]Peter the Great St. Petersburg Polytechnical University, 29 Polytechnicheskaya str., 195251, St. Petersburg, Russia;
[3]Saint-Petersburg National Research University of Information Technologies, Mechanics and Optics, 49 Kronverkskiy pr., 197101, St. Petersburg, Russia;
[4]Laboratory of Photonics, Tampere University of Technology, Tampere, Finland.
**Corresponding author: korobkotam@rambler.ru*

We experimentally demonstrate a harmonically mode-locked Er-doped fiber laser. The distinctive feature of the laser is highly stable pulse trains generated via self-starting hybrid mode-locking triggered by frequency-shifting and nonlinear polarization evolution. A intra-cavity tunable bandpass filter allows getting a pulse repetition rate up to 12 GHz with local adjustment of the wavelength.

Keywords: fiber lasers; harmonic mode-locking; high-repetition pulse trains.

1. Introduction

Laser sources with high-repetition-rate pulses are in demand in a wide range of photonics-based applications. Notably, they have been applied in the fields of optical communications, ultrafast optics, optical frequency metrology and microwave photonics [1, 2]. Harmonic mode-locking (HML) soliton fiber lasers exhibiting advantageous consumer properties, such as compactness, reliability, low cost and convenience of beam delivery approach are among the most attractive alternatives for high-repetition-rate sources [3, 4].

Various mechanisms could be responsible for the HML implementation in fiber lasers. They can be classified based on an actual mode-locking mechanism (nonlinear polarization rotation (NPR), special saturable absorbers such as carbon nanotubes, semiconductor mirrors, etc.) and determination of the physical effects leading to periodic pulse arrangement in a laser cavity. The key element of HML laser configurations comprising an intra-cavity periodic filter is built-in etalon with a free spectral range (FSR) equal to the pulse repetition rate [5]. In this case, the required condition of multi GHz pulse train generation is high Q-factor of the etalon allowing to select individual modes from thousands laser cavity modes [6]. In turn, another option of passive HML implies the formation of strongly periodic pulse arrangement in a laser cavity induced by repulsion forces between the pulses [7]. The repulsion could be caused by interaction through saturating and relaxing dissipative parameters [8, 9], interaction through continuous-wave (CW) radiation component or dispersion waves [10] or interaction through acoustic waves induced by

electrostriction [11]. Determining of the pulse interaction scheme for some HML fiber lasers remains questionable, so often only the mode-locking mechanism is mentioned in laser specification. For example, NPR harmonically mode-locked fiber lasers, which are able to scale pulse repetition rates up to 20 GHz [12], and multi-GHz fiber lasers on the base of carbon nanotubes or graphene saturable absorbers [13, 14] have been reported. The main quality factors of the pulse train are the supermode suppression level (SSL) and principally connected with it timing jitter [15]. The SSL of 40-50 dB is reported for fiber laser based on carbon nanotubes or graphene saturable absorbers [13, 16]. The NPR harmonically mode-locked fiber lasers demonstrate the slightly lower SSL about ~ 30 dB and it decreases with repetition rate (down to ~ 15-25 dB at maximal repetition rates ~ 20 GHz) [12].

Recently, hybrid HML fiber lasers with cooperative action of NPR and frequency shifting produced by optical modulator have attracted considerable interest [17]. Important to note that in this case the modulator frequency is much lower than the pulse repetition rate, i.e. not the active but the passive harmonic mode-locking with soliton frequency shifting effect occurs. Later, it was proved theoretically [18] that this cooperative effect can be applied to improve the stability of HML lasers by decreasing the specific timing jitter originated from the negative correlations between energy fluctuations of different pulses [19]. The frequency shifting allows reduction of these negative correlations of fluctuations simultaneously maintaining the positive correlations arising from a slow dynamic of gain and leading to periodic pulse arrangement and successful harmonic mode-locking. So, the hybrid scheme combining the NPR mode-locking and frequency shifting is promising for demonstration of HML lasers with high repetition rate and improved stability. Besides that, as far as we know similar hybrid HML fiber lasers with repetition rate more than 1 GHz are not reported yet.

Important soliton laser property manifested at the multiple pulse generation is energy quantization effect ensuring the equivalence of all pulses [20]. This effect leads to an increase in the pulse number in the cavity with the pump and for HML lasers supporting the regular pulse arrangement results in ability to control the repetition rate by the pump power. There is another way to manage the repetition rate without heavy pumping due to control of the single pulse energy for example through the change of the gain bandwidth. Gain narrowing leads to the reduction of the individual pulse spectrum width and energy that results in an increase of pulse number in the cavity and growth of the repetition rate. At the same time, an increase in the pulse duration and decrease in the peak soliton power should be attributed to negative aspects of this method.

All observations mentioned above motivated the study of soliton HML fiber laser with NPR and frequency shift providing hybrid mode-locking scheme. The main objective of the work is to get the multi-GHz pulse repetition rates by introducing a special filter into the cavity to control the gain bandwidth. The proposed method allows maintaining the high quality of pulse train (high SNR and SSL) at high order HML avoiding heavily pumping.

2. Experimental setup

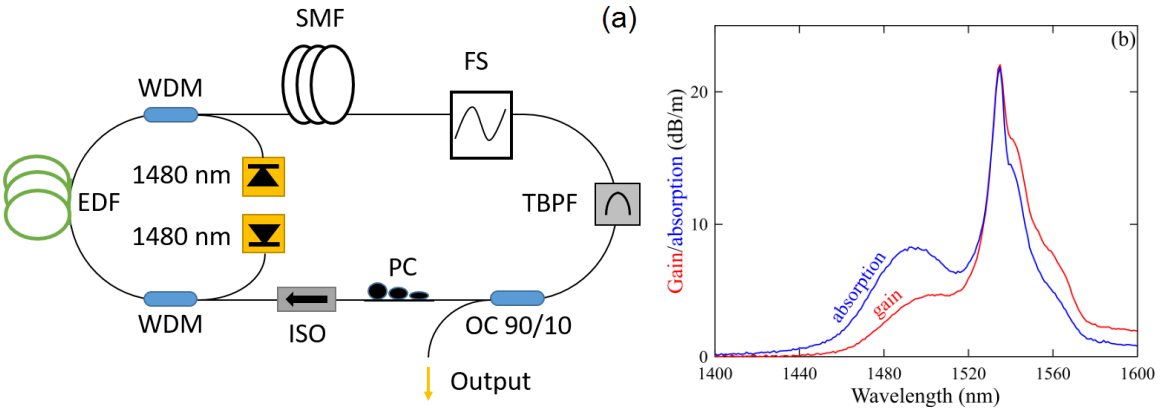

Fig.1. (a) Scheme of HML fiber laser. PC –polarization controller, FS - acousto-optic modulator with frequency shifting, TBPF – tunable bandpass filter, OC –output coupler, ISO- optical isolator, EDF - Er-doped fiber, SMF-single-mode fiber, WDM- wavelength-division multiplexer. (b) Absorption/gain curves for EY-305 active fiber used in the experiment.

The experimental setup of the fiber laser is shown in Fig.1 (a). The fiber ring cavity consists of 5.75-m long erbium-doped fiber (EDF – EY-305) as a gain medium with the dispersion D = 9 ps/(nm km) that is pumped by two CW laser pump diodes at 1480 nm with a maximum pump power of 550 mW each. The absorption/gain curves for the EDF are shown in Fig. 1 (b). The EDF length has been optimized to achieve enough gain and reach high-order HML. Two 1480/1550 multiplexers (WDM) are spliced on both sides of the gain medium for pump light delivering. The whole cavity length is L=64.92 m, which corresponds to the fundamental cavity frequency of 3.19 MHz. All fiber components of the scheme are made with standard telecom single-mode fiber SMF-28 (D = 18 ps/(nm km) at 1550 nm). Unidirectional laser emission is ensured by a fiber optical isolator. The output coupling of generated light equaled to 10% is carried out by an output coupler (90/10). An acousto-optic modulator (AOM MT80-IIR30-Fio-PM0.5) included into the cavity operates as a frequency shifter with the shift $\Delta\nu = 80$ MHz. AOM is the only polarization-sensitive element of the cavity with polarization extinction ratio ~ -20 dB. It's important to note that the frequency shifter and its polarization-maintaining pigtails are the parts of the Lyot filter formed into the cavity and leading to some specific features of the oscillator's spectrum. An additional control element also included into the fiber laser cavity is a

tunable bandpass filter (TBPF) OZ Optics (BTF-11-11-1525/1570), which allows filtering the signal by adjusting the bandwidth and tuning the central wavelength within the band of 1525-1570 nm. During the experiments, the filter bandwidth was set to the value close to the minimum (slightly more than 1 nm). The special feature of OZ Optics BTF is polarization insensitivity.

The output spectra of the laser were measured by optical spectrum analyzer Ando AQ6317B with 0.02 nm resolution. The RF spectrum analyzer Tektronix RSA607A coupled with 15-GHz-bandwidth photodetector UPD-15-IR2-FC (for pulse repetition rates up to 7.5 GHz) and fast digital oscilloscope Keysight UXR0204A coupled with 33-GHz-bandwidth photodetector Keysight (for pulse repetition rates above 7.5 GHz) were used to monitor the RF signals. Autocorrelation traces were recorded by scanning autocorrelator FR103-WS.

3.Results

The experimental results were obtained by tuning the central wavelength of the TBPF in the band of 1528 – 1548 nm. Mode-locking at the fundamental frequency (3.19 MHz) occurs in the whole tuning range of TBPF when the total pump power exceeds 200 mW. With further increase of the pump power the laser moves to operation in multiple pulse generation with a periodic distribution of pulses into the cavity, i.e. it demonstrates the HML. The HML pulse trains with various maximal repetition rates are observed in the whole tuning range of TBPF. The spectra of pulse trains with the highest obtained repetition rates are shown in Fig. 2. The specific two-humped structure of the spectra is caused by the Lyot filter formed in frequency shifter [21]. Besides that, the combined effect of the TBPF and Lyot filter leads to some variations of the spectrum's bandwidth observed in the whole range of 1528 – 1548 nm.

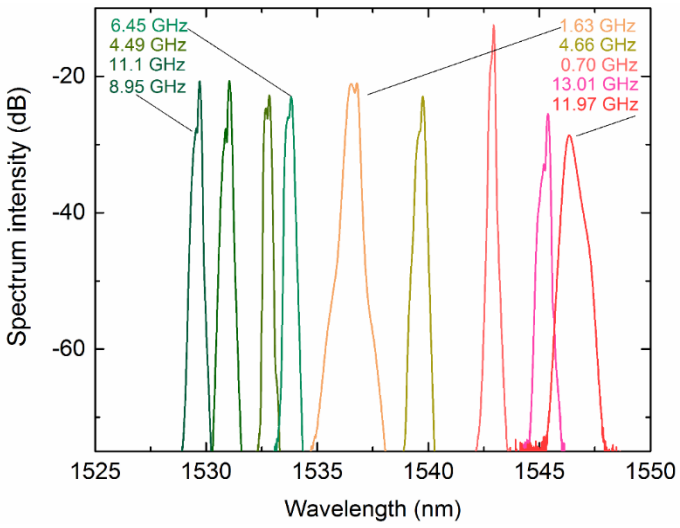

Fig.2. The optical spectra of generated pulse trains depending on the central wavelength of the tunable filter. Spectra are shown with the mark of maximum repetition rates obtained in each bandpass region.

The laser operation within the tuning range of TBPF can be divided into two specific bands: short- and long- wavelength. In the short-wavelength band (1528-1535 nm) the mode-locked regime is characterized by high stability. The pulsed operation initiated by adjusting the PC orientation at a low repetition rate is maintained with increasing the pump power without interruption. The pulse repetition rate, as well as the output power, increases proportionally to the pump without the requirement of additional polarization adjustment. Figs.3 (a) shows the changing of laser parameters (average output power and repetition rate) at the central wavelength of the filter $\lambda_0 = 1533.7$ nm depending on pump power in the short-wavelength band. The dependence revealed the nearly linear character for the entire range of the pump rate for both parameters. Fig. 3 (b) presents the evolution of output optical spectra with pump increase and corresponding growth of the repetition rate. The spectra recorded for two different central wavelengths λ_0 of the filter to demonstrate similar performance within the operational band. In addition to the specific two-humped structure of the spectra, one can notice some deformations of the spectrum's shape accompanying the repetition rate change that can be explained by variations of NPR-induced cavity transmission.

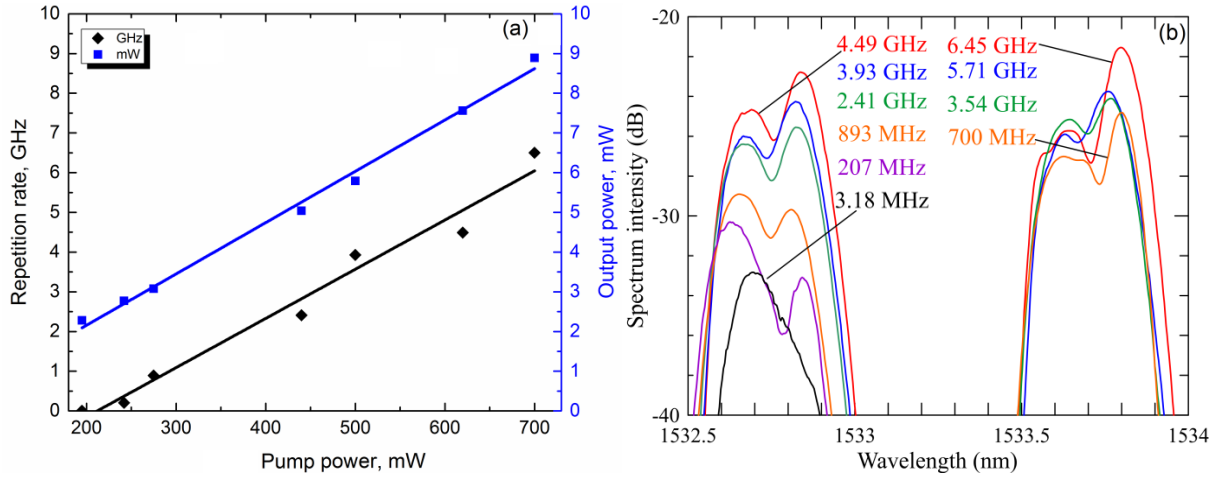

Fig. 3. (a) Dependence of output power and pulse repetition rate on the pump power at the central wavelength of the filter $\lambda_0 = 1533.7$ nm. (b) The optical spectra of generated pulse trains at different repetition rates for two central wavelengths of the TBPF $\lambda_0 = 1532.7$ nm and $\lambda_0 = 1533.7$ nm.

To determine the temporal shape of the pulse, the measurement of autocorrelations were performed for pulse trains with fundamental repetition rate (3.18 MHz) and high order HML (4.49 GHz) generated at the central wavelength of the filter $\lambda_0 = 1532.7$ nm (Figs. 4 (a, b)). The pedestal-free autocorrelations traces were well fitted to sech^2-shape in both cases. The temporal

full widths at half-maximum (FWHM) of the autocorrelation traces were 19.5 ps and 15.5 ps respectively, so the corresponding pulse durations were estimated to be 12.7 ps and 10.1 ps. The 3dB pulse spectrum widths were estimated as 0.195 nm (~25 GHz) and 0.28 nm (~36 GHz) respectively. The time-bandwidth products were approximately 0.32 and 0.365, so in both cases, the pulses can be considered as transform-limited solitons.

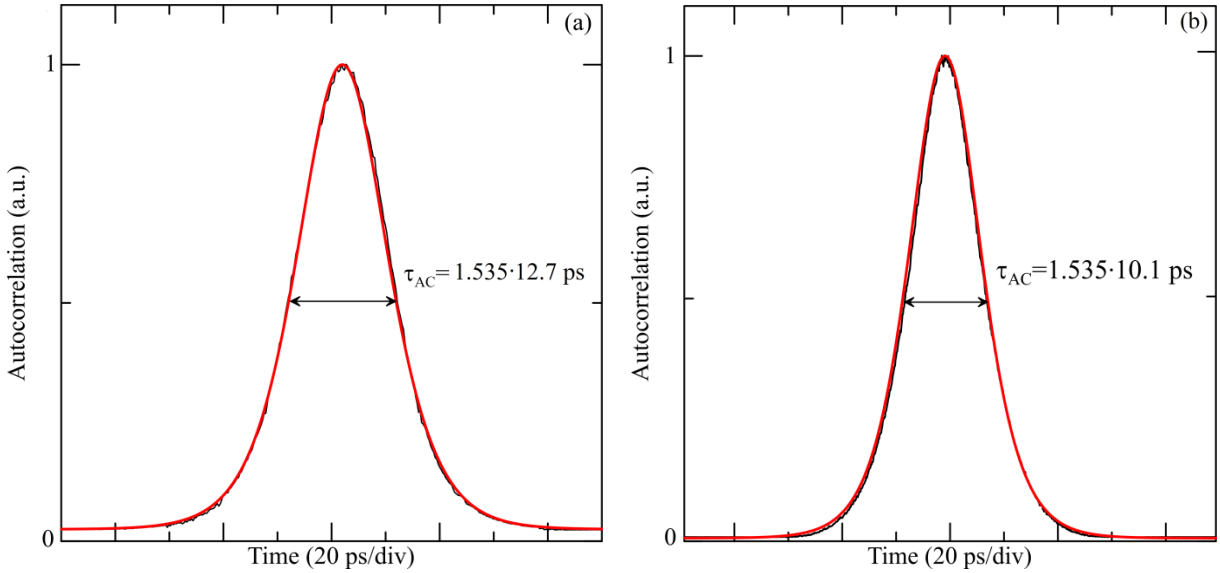

Fig. 4. Autocorrelation traces of pulses generated at the central wavelength of the filter $\lambda_0 = 1532.7$ nm: (a) for the pulse train with fundamental frequency 3.18 MHz, (b) for the pulse train with a repetition rate of 4.49 GHz. The red lines show the sech^2 fitting.

The mode-locked operation demonstrated valuable robustness against external perturbations. In experiments, the free-running laser maintained stable HML for more than 1 hour without any adjustment. We performed the critical analysis of the laser stability by means of its RF spectra, which were recorded for all pulse trains obtained within the short-wavelength band. Fig. 5 (a) demonstrates an example of the RF spectra represented the pulse train with a repetition rate of 4.49 GHz at a central wavelength of the TBPF $\lambda_0 = 1532.7$ nm. The spectra were recorded with different resolution. The RF spectrum with the span range equaled to 30 kHz and measured with fine resolution of 30 Hz (Fig. 5 (a), inset) indicates high signal-to-noise ratio (S/N) >60 dB, which suggests good train stability within the fundamental period of the laser cavity T. The quantitative estimation of the corresponding low-frequency jitter can be performed as: $\Delta t/T = (1/2\pi)(\Delta P \Delta f / \Delta f_{res})^{1/2} < 0.05\%$ [15], where ΔP is the pedestal to signal-peak power ratio, Δf is the width of the pedestal and Δf_{res} is the resolution of the spectrum analyzer for the measurement. The RF spectrum with a resolution of 1 kHz indicates the sequence of supermode noise peaks spaced apart by a fundamental frequency 3.18 MHz that is the typical feature of

HML lasers caused by the correlations between pulses inside the cavity [19]. It's important to note that the measured supermode suppression level (SSL) of this pulse train is higher than 35 dB corresponding to the most stable HML lasers with NPR mode-locking [12]. The large-scaled RF spectrum (Fig. 5 (b)) shows two harmonics of the repetition rate equaled to 4.49 GHz without additional spectral modulation indicating lack of instabilities. Similar RF spectra are recorded for other pulse trains. The SSL and S/N values obtained from these RF spectra for the central wavelength of the TBPF $\lambda_0 = 1532.7$ nm are summarized in Fig. 6 as a function of the pulse repetition rate. One can see that these parameters are relatively similar for any repetition rates confirming similar level of stability for generated pulse trains. It is worth mentioning again that the results shown in Fig. 6 were obtained only by the manipulation of the pump power without any changing of polarization settings.

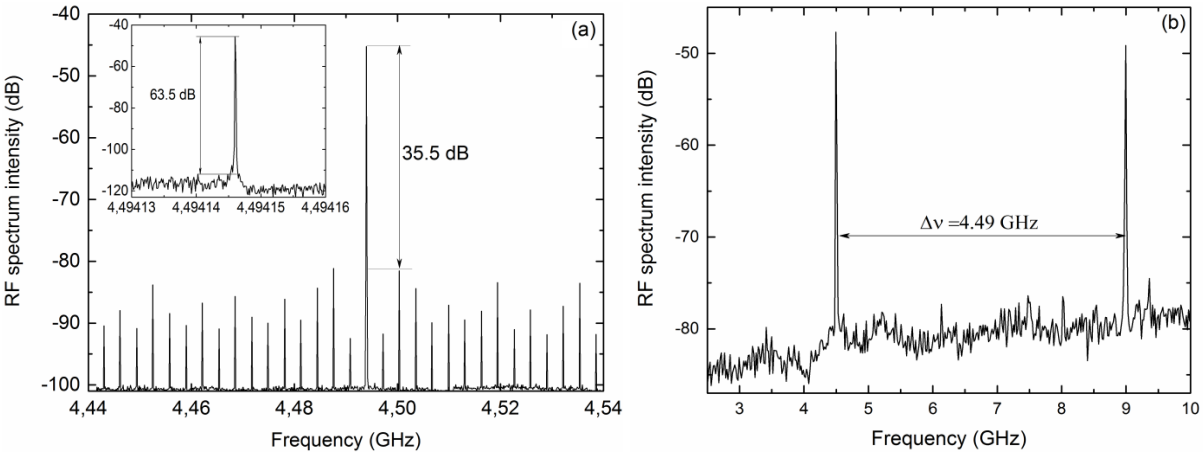

Fig. 5. The recorded RF spectra of the pulse train with a 4.49 GHz repetition rate at the central wavelength of the filter $\lambda_0 = 1532.7$ nm. (a) RF spectrum in a 100 MHz span (resolution 1 kHz); inset: the RF spectrum in a 30 kHz span (resolution 30 Hz). (b) RF spectrum with two harmonics of the repetition rate (resolution 200 kHz).

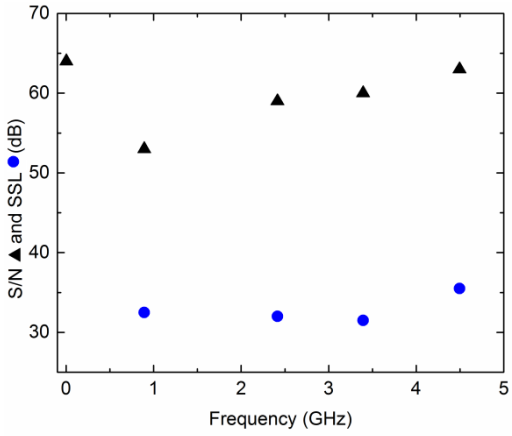

Fig. 6. The signal-to-noise ratio (black triangles) and the SSL (blue circles) at different repetition rates of the pulse trains measured for the central wavelength of the filter $\lambda_0 = 1532.7$ nm.

The measurements show that the pulse trains generated at the long-wavelength band (1535-1548 nm) of the TBPF are generally less stable. At some value of the central wavelength of the TBPF

(right side in Fig.2) the HML generation with high repetition rate (> 1 GHz) is occurred, however, these regimes are not stable against the pump power change. In contrast to the previous case, the laser responds to the pump change not by adjusting the pulse repetition rate, but with the disruption of mode-locking. To restore the mode-locking with any pump changing additional adjustment of the polarization controller is necessary. Nevertheless, just in this tuning range of the TBPF, the HML with pulse repetition rates more than 10 GHz is achieved. At a central wavelength of the TBPF $\lambda_0 = 1546.5$ nm and the total pump power of 590 mW the HML with repetition rate 11.97 GHz and SSL > 40 dB is detected (Fig. 7 – middle row). 13.01 GHz pulse repetition rate is obtained at the central wavelength of the TBPF $\lambda_0 = 1545.5$ nm with pump power equal to 538 mW, but the form of RF spectrum and essentially low SSL indicate a lack of pulse train stability (Fig. 7– the top row). In comparison, Fig.7 also shows the oscilloscope waveform and the RF spectrum of the pulse train with a repetition rate of 8.95 GHz obtained in the short-wavelength tuning range of the filter ($\lambda_0 = 1529$ nm – bottom row).

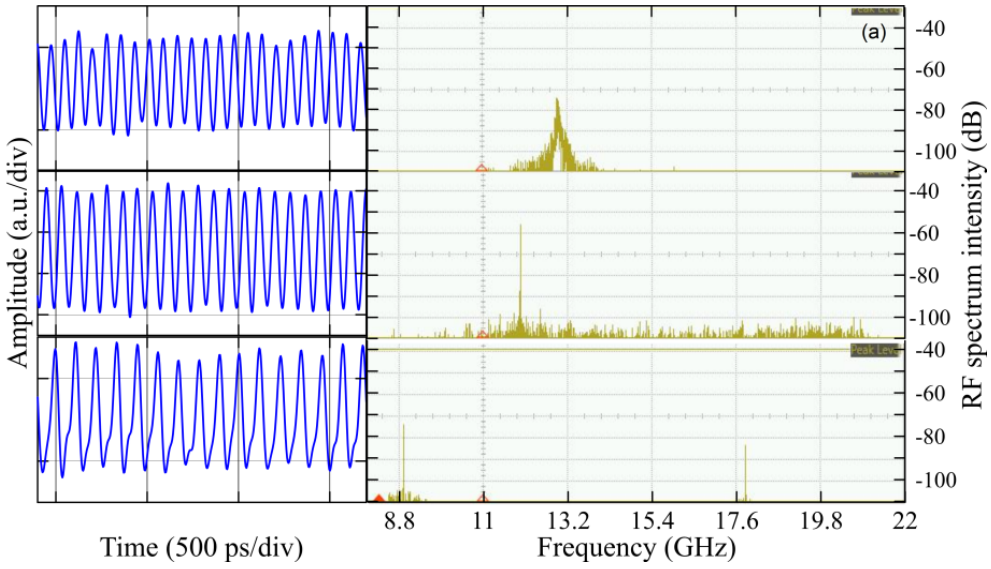

Fig. 7. Oscilloscope traces (on the left) and RF spectra (on the right) of pulse trains with repetition rates 8.95, 11.97 and 13.01 GHz at central wavelengths of the TBPF $\lambda_0 = 1529$ nm, 1546.5 nm and 1545.5 nm (from bottom to top) respectively.

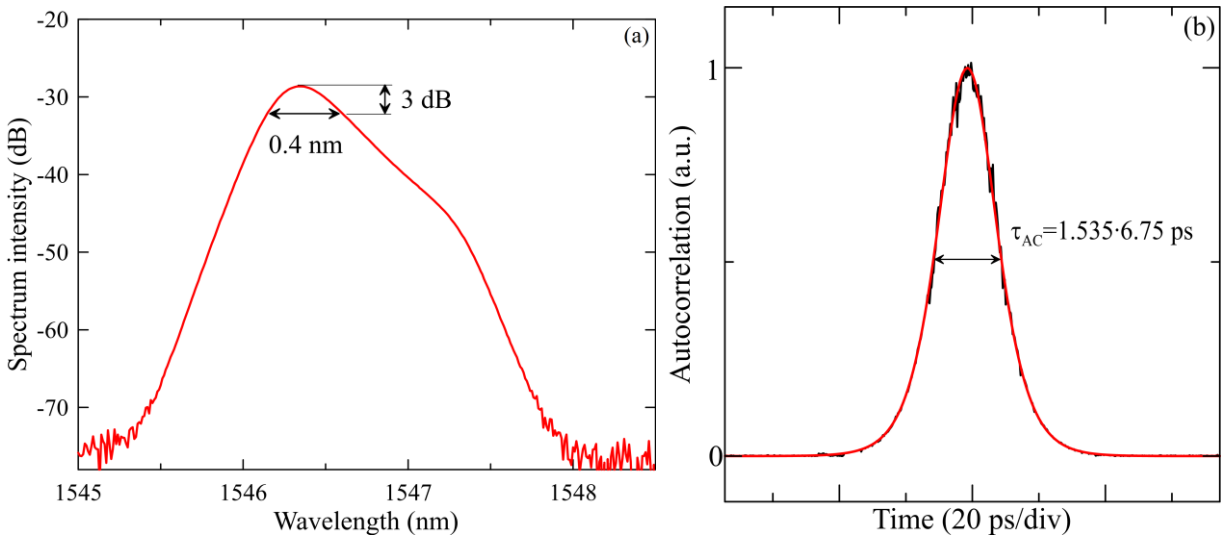

Fig.8. (a) The optical spectrum and (b) autocorrelation trace of the pulse generated at the central wavelength of the filter $\lambda_0 = 1546.5$ nm for the repetition rate of 11.97 GHz. The red line on (b) shows the sech^2 fitting.

Fig 8 (a) shows the optical spectrum and Fig. 8 (b) shows the measured autocorrelation trace of the single pulse generated at the central wavelength of the filter $\lambda_0 = 1546.5$ nm for the repetition rate of 11.97 GHz. As in the previous case of the short-wavelength band, the autocorrelation is well fitted to the sech^2 pulse shape. Temporal FWHM of the autocorrelation trace is 10.35 ps and the corresponding FWHM pulse width is approximately 6.75 ps. The 3 dB pulse spectrum width is 0.4 nm (~ 50 GHz), so the pulse is also transform-limited soliton that is confirmed by the time-bandwidth product approximately equaled to 0.34.

4. Discussion and conclusions

The most important feature of the considered laser scheme is harmonic mode-locking supported at any multi-pulse generation regime. This observation means that there is a stable inter-pulse repulsive force ensuring uniform periodic pulse distribution in the fiber ring cavity. A variety of mechanisms have been suggested as interaction mechanisms between pulses in passive harmonically mode-locked lasers. These mechanisms are direct soliton-soliton, soliton-dispersive wave interactions, pulse interaction through acoustic waves and interaction through gain depletion and recovery (GDR). Kutz and coauthors [8] show that the last mechanism is the most probable source of the repulsion source. In our experiments, we observe that the laser generates transform-limited solitons with durations of about 10 ps. For the pulse train with repetition rate ~ 0.1–10 GHz the interpulse distance is many times greater than the pulse duration and direct soliton interaction should be excluded from the origin of repulsion. Frequency shift followed by the filtering of laser radiation suppresses the possible generation of CW radiation

component. This assumption confirmed by the shape of the optical spectrum eliminates the interaction through CW-component and dispersion waves from possible repulsion forces. The fact that a stable HML regime is available for a wide range of repetition rates also excludes transverse acoustic wave excitation mechanism as a mechanism responsible for laser stabilization [22]. Consequently, we can conclude that the reason for the repulsion forces is the interaction through the GDR.

The considered laser can possess two types of saturable absorption mechanism necessary for mode-locking: i) NPR and ii) frequency shifting followed by the spectrum filtering that is the basis of so-called frequency shifted feedback (FSF) lasers [23, 24]. Analysis of output power and pulse repetition rate changes with the pump at a given setting of PC orientation (Fig 3 (a)) shows that the pump increasing leads to generation of new pulses with approximately constant energy $E_p = W_{out}/\nu_{rep}$. The main pulse parameters such as spectrum width and peak power do not change significantly in a wide range of repetition rates that is verified by only minor modifications of the pulse spectrum width (Fig 3 (b)) and pulse duration (Figs. 4 (a, b)). Besides that, we should note that a slight rotation of the PC leads to a little reduction of the maximal pulse repetition rate achieved at this pump. All these observations correspond to the standard model of multi-soliton generation [20] and allow us to conclude that the laser demonstrates NPR mode-locking with the frequency shifting represented as a small perturbation. Assuming that, repulsion forces and the HML implementation are provided by above mentioned GDR [8], we consider the frequency shift and filtering as the mechanism for stabilization of the HML pulse train and decrease of the noise level [18]. Besides the fact that this mechanism suppresses CW-component and dispersion waves, results of the Ref. [18] show that the frequency shift and filtering included as small perturbations in the scheme with NPR harmonic mode-locking, which established through GDR, provides the additional mechanism for the pulse unification and stabilization of interpulse distances [25]. However, it should be noted that the successful HML is possible only when all these dissipative mechanisms (GDR, NPR mode-locking, frequency shift and filtering) are balanced and stabilizing forces exceed the destructive noise effect. This rather complex balance occurs only in a certain range of pulse parameters, for example, in a certain range of pulse peak power and spectrum bandwidth. In the short-wavelength band, the large parameter variation area allows achieving the HML in a broad range of repetition rates. At displacement, to the long-wavelength band, the pulse parameters necessary to balance these dissipative mechanisms are substantially changed. (Note that the duration of the pulse mode-locked at central wavelengths of the TBPF $\lambda_0 = 1546.5$ nm is significantly less than the duration of pulses at $\lambda_0 = 1532.7$ nm). As a result, the range of possible pulse parameters is extremely

reduced that corresponds to the sudden changes in the lasing properties, when scanning the right part of laser spectral band. Nevertheless, in the long-wavelength band of the filter the pulse train with repetition rate of ~ 12 GHz and SSL level> 40 dB is observed after fine adjusting of the PCs and pump power. This fact can be interpreted as exact selection of the pulse parameter providing the necessary balance of all dissipative forces in the laser system.

In conclusion, we should note that the proposed experimental scheme is promising for the generation of stable and low noise high-repetition-rate pulse trains with the possible tuning of the repetition rate and local adjustment of the wavelength. The application of frequency shifter and tunable filter with a small (~ 1 nm) passband allows getting the HML with a repetition rate more than 10 GHz and SSL greater than 35 dB, while the generation of CW component and dispersion waves is completely suppressed. The disadvantages of the method involve the relatively long duration (~ 10 ps) and low energy (~ 1.5 pJ) of the generated pulses, however, the proposed laser source can easily be included in cascade amplifying schemes, increasing the pulse energy by orders of magnitude [26, 27].

This work was supported by the Russian Science Foundation (19-72-10037), the Russian Foundation for Basic Research (19-42-730009) and the Academy of Finland Flagship Programme, Photonics Research and Innovation (PREIN) (320165).

References

1. Haus, H. A., & Wong, W. S. (1996). Solitons in optical communications. *Reviews of modern physics*, *68*(2), 423.
2. A. Schliesser, N. Picqué, T.W. Hänsch, "Mid-infrared frequency combs,"Nature Photonics, **6**, 440-449 (2012).
3. Fermann, M. E., & Hartl, I. (2013). Ultrafast fibre lasers. *Nature Photonics*, *7*(11), 868.
4. Chernysheva, M., Rozhin, A., Fedotov, Y., Mou, C., Arif, R., Kobtsev, S. M., ... & Turitsyn, S. (2017). Carbon nanotubes for ultrafast fibre lasers. *Nanophotonics*, *6*(1), 1-30.
5. Mao, D., Liu, X., Sun, Z., Lu, H., Han, D., Wang, G., & Wang, F. (2013). Flexible high-repetition-rate ultrafast fiber laser. *Scientific reports*, *3*, 3223.
6. Korobko, D. A., Fotiadi, A. A., & Zolotovskii, I. O. (2017). Mode-locking evolution in ring fiber lasers with tunable repetition rate. *Optics express*, *25*(18), 21180-21190.
7. Grudinin, A. B., & Gray, S. (1997). Passive harmonic mode locking in soliton fiber lasers. *JOSA B*, *14*(1), 144-154.
8. Kutz, J. N., Collings, B. C., Bergman, K., Knox, H., "Stabilized pulse spacing in soliton lasers due to gain depletion and recovery," IEEE Journal of Quantum Electronics 34 (9), 1749-1757 (1998).
9. D. A. Korobko, O. G. Okhotnikov, I. O. Zolotovskii, "Long-range soliton interactions through gain-absorption depletion and recovery," Optics letters, **40**(12), 2862-2865 (2015).
10. Semaan, G., Komarov, A., Salhi, M., & Sanchez, F. (2017). Study of a harmonic mode lock stability under external continuous-wave injection. *Optics Communications*, *387*, 65-69.

11. Dianov, E. M., Luchnikov, A. V., Pilipetskii, A. N., & Starodumov, A. N. (1990). Electrostriction mechanism of soliton interaction in optical fibers. *Optics letters*, *15*(6), 314-316.
12. Lecaplain, C., & Grelu, P. (2013). Multi-gigahertz repetition-rate-selectable passive harmonic mode locking of a fiber laser. *Optics express*, *21*(9), 10897-10902.
13. Sobon, G., Sotor, J., & Abramski, K. M. (2012). Passive harmonic mode-locking in Er-doped fiber laser based on graphene saturable absorber with repetition rates scalable to 2.22 GHz. *Applied Physics Letters*, *100*(16), 161109.
14. Sun, Z., Hasan, T., & Ferrari, A. C. (2012). Ultrafast lasers mode-locked by nanotubes and graphene. *Physica E: Low-dimensional Systems and Nanostructures*, *44*(6), 1082-1091.
15. D. von der Linde, "Characterization of the noise in continuously operating mode-locked lasers," Appl. Phys. B 39(4), 201–217 (1986)
16. Mou, C., Arif, R., Rozhin, A., & Turitsyn, S. (2012). Passively harmonic mode locked erbium doped fiber soliton laser with carbon nanotubes based saturable absorber. *Optical Materials Express*, *2*(6), 884-890.
17. Noronen, T., Okhotnikov, O., & Gumenyuk, R. (2016). Electronically tunable thulium-holmium mode-locked fiber laser for the 1700-1800 nm wavelength band. *Optics express*, *24*(13), 14703-14708
18. Gumenyuk, R. V., Korobko, D. A., & Zolotovskii, I. O. (2020). Stabilization of passive harmonic mode locking in a fiber ring laser. *Optics Letters*, *45*(1), 184-187.
19. Rana F, Lee HL, Ram RJ, Grein ME, Jiang LA, Ippen EP, Haus HA. Characterization of the noise and correlations in harmonically mode-locked lasers. JOSA B, 2002 19(11):2609-21.
20. Tang, D. Y., Zhao, L. M., Zhao, B., & Liu, A. Q. (2005). Mechanism of multisoliton formation and soliton energy quantization in passively mode-locked fiber lasers. *Physical Review A*, *72*(4), 043816
21. Zeng, Y., Fan, W., Zhang, S., & Wang, X. (2020). The effects of Lyot filter on the SNR of mode-locked fiber laser. *Optics & Laser Technology*, *128*, 106148.
22. Gray, S., Grudinin, A. B., Loh, W. H., & Payne, D. N. (1995). Femtosecond harmonically mode-locked fiber laser with time jitter below 1 ps. *Optics letters*, *20*(2), 189-191
23. Sousa, J. M., & Okhotnikov, O. G. (2000). Short pulse generation and control in Er-doped frequency-shifted-feedback fibre lasers. *Optics communications*, *183*(1-4), 227-241.
24. Gumenyuk, R., Korobko, D. A., Zolotovsky, I. O., & Okhotnikov, O. G. (2014). Role of cavity dispersion on soliton grouping in a fiber lasers. *Optics express*, *22*(2), 1896-1905.
25. Wabnitz, S., Kodama, Y., & Aceves, A. B. (1995). Control of optical soliton interactions. Optical Fiber Technology, 1(3), 187-217.
26. Kotov, L., Likhachev, M., Bubnov, M., Medvedkov, O., Lipatov, D., Guryanov, A., ... & Février, S. (2015). Millijoule pulse energy 100-nanosecond Er-doped fiber laser. Optics Letters, 40(7), 1189-1192.
27. Stolyarov, D. A., Korobko, D. A., Zolotovskii, I. O., & Sysolyatin, A. A. (2019). A Laser Complex with a Central Wavelength of 1.55 μm for Generation of Pulses with Energy Exceeding 1 μJ and a Supercontinuum Spanning a Nearly Two-Octave Range. Optics and Spectroscopy, 126(6), 638-644.